Since January 2020 Elsevier has created a COVID-19 resource centre with free information in English and Mandarin on the novel coronavirus COVID-19. The COVID-19 resource centre is hosted on Elsevier Connect, the company's public news and information website.

Respiratory Medicine 168 (2020) 105989

Contents lists available at ScienceDirect

Respiratory Medicine

journal homepage: http://www.elsevier.com/locate/rmed

Association between chest CT features and clinical course of Coronavirus Disease 2019

Zhibing Luo [a,1], Na Wang [a,1], Ping Liu [b,1], Qian Guo [a,1], Linyu Ran [a], Feilong Wang [a], Yuling Tang [b,**], Qiang Li [a,*]

[a] Respiratory and Critical Care Center, Shanghai East Hospital Affiliated by Tongji University, China
[b] Respiratory Medical Center, First Hospital of Changsha, Hunan Province, China

ARTICLE INFO

Keywords:
Coronavirus disease
Computed tomography
SARS-CoV2
Viral infection

ABSTRACT

Purpose: This retrospective study aims to illustrate the radiographic characteristics of Coronavirus Disease 2019 and the correlation with the clinical course.

Methods: 195 hospitalized patients confirmed as Coronavirus Disease 2019 at First Hospital of Changsha, Hunan Province from December 31, 2019 to February 20, 2020 were enrolled. Chest computed tomography scan, clinical data and laboratory tests results were collected accordingly. Variable characteristics were recorded, radiographic evolution and outcome were analyzed along with the time course. Representative laboratory tests results were analyzed based on the image findings.

Results: Majority of the patients showed bilateral (73.8%), multiple lobes involvements (75.9%), peripheral distribution (83.1%), ground-glass opacification (41.0%), increased vascular margins (63.1%), long axis parallelism (55.9%), patchy ground-glass opacities beneath the pleura (51.3%) and consolidation (45.6%). According to the repeated radiology analysis, patients of improving/stable group tended to have younger age compared with worsening group (45.3 ± 15.0 VS. 59.3 ± 13.5, $P = 0.001$). Based on the laboratory test results, patients with positive image findings shared elder age, 46.0 (35.0–60.0)VS.31.0 (12.0–37.0) $P < 0.001$, and higher chance developing fever($P < 0.05$); higher level of lymphocytes, C-reactive protein, erythrocyte sedimentation rate and lactate dehydrogenase; lower level of white blood cells, neutrophil and albumin($P < 0.001$).

Conclusions: There are several specific image changes along with the disease progression may be helpful in early recognition and differential diagnosis of Coronavirus Disease 2019. Comprehensive assessments of both imaging feature and laboratory test results may offer an intact knowledge of Coronavirus Disease 2019.

1. Introduction

Since the initial report of the newly-emerging novel coronavirus pneumonia in December 2019 from Wuhan, China [1], which is now defined as Coronavirus Disease 2019 (COVID-19) caused by severe acute respiratory syndrome coronavirus 2 (SARS-CoV-2) [2], the confirmed population reached up to 83,428 in China and 2,158,033 globally by April 16,2020 [3]. WHO has increased the assessments of the spreading and impact risk of COVID-19 to very high risk at the global level due to rapid increase of cases internationally including Italy, United States, Spain and Germany, etc. [4].

Most of the cases had travelling or contact history of China or Wuhan or contact history with people from China, but cases without any travelling or contact history has been reported recently suggesting possible local transmission. Transmission of COVID-19 is believed via close contact, aerosol and respiratory droplets from cough and sneezes [5]. However, detection of SARS-CoV-2 virus RNA from eye discharge, saliva, urine, blood and stool specimens were also reported accordingly, indicating more investigations are required [6].

The most common symptoms of COVID-19 are non-specific including fever, cough, dyspnea, shortness of breath, and fatigue [7]. Some cases may rapidly progress to severe pneumonia, respiratory failure, multi-organ dysfunction and even death [8]. Gastrointestinal symptoms such as nausea, vomiting, diarrhea and asymptomatic cases have also been described [9,10], though relatively rare. Radiographic tests

* Corresponding author. No.150 Jimo Road, Pudong District, Shanghai, 200020, China.
** Corresponding author. No. 311 Yingpan Road, Kaifu District, Changsha, Hunan Province, China.
E-mail addresses: tyl71523@sina.com (Y. Tang), liqressh@hotmail.com (Q. Li).
[1] Zhibing Luo, Na Wang, Ping Liu, and Qian Guo contributed equally to this work.

https://doi.org/10.1016/j.rmed.2020.105989
Received 13 April 2020; Received in revised form 19 April 2020; Accepted 20 April 2020
Available online 22 April 2020

Abbreviation

ARDS	acute respiratory distress syndrome
ACE2	angiotensin-converting enzyme 2
COVID-19	Coronavirus Disease 2019
CT	computed tomography
CBC	complete blood cell
CRP	C-reactive protein
ESR	erythrocyte sedimentation rate
GGO	ground-glass opacification
GGN	ground-glass nodule
LDH	lactate dehydrogenase
LAD	lymphadenopathy
PCR	polymerase chain reaction
SARS-CoV-2	severe acute respiratory syndrome coronavirus 2

especially chest computed tomography (CT) scan showed several abnormalities strongly favor the diagnosis of COVID-19 including bilateral peripheral ground-glass opacities, consolidation and linear opacities in most cases [11].

SARS-CoV-2 virus is now identified as a member of *Betacoronavirus* genera of coronavirnae family [12], which is characterized as positive-sense single-strand RNA (+ssRNA) virus [13].The definitive diagnosis relies on positive detection of viral RNA nucleic acid amplification tests (polymerase chain reaction, PCR) [14] of specimens either from upper respiratory tract (nasopharyngeal and oropharyngeal swab) or lower respiratory tract (sputum, tracheal aspirate, or bronchoalveolar lavage) [15]. Because of the high specificity but poor sensitivity of nucleic acid test, false negative cases are frequently reported. Thus, acquaintance the radiographic characteristics of COVID-19 lungs is crucial in terms of the early identification, differential diagnosis, staging as well as subsequent management strategies.

In this retrospective study, we collected chest CT scan data of 195 cases and clinical characteristics in 187 case of them in First Hospital of Changsha, Hunan Province from December 31, 2019 to February 20, 2020, aiming to describe the CT scan characteristics of COVID-19 and investigate the relationship between the clinical manifestation and radiographic features.

2. Materials and methods

2.1. Patients population

195 hospitalized patients in First Hospital of Changsha, Hunan Province from December 31, 2019 to February 20, 2020 were enrolled and the clinical and laboratory tests data were collected accordingly. The First Hospital of Changsha, capital city of Hunan province with 8.15 million population, also known as Public Health Treatment Center of Changsha, is the only designated hospital for admission and management of COVID-19 patients from Changsha and surrounding area. All of the patients were confirmed of COVID-19 via positive detection of SARS-COV-2 RNA by PCR.

2.2. Methods

CT scan was performed with supine position during a single breathhold on a Siemens Go Top 64 scanner (Siemens Healthineers, Germany) and a GE Brivo CT325 scanner (GE Healthcare, United States) respectively. For CT acquisition, the voltage was 120 kVp and tube current was 350 mA, and the slice thickness of the reconstruction was 5 mm. Repeated CT scan were performed in 95 patients 3–6 days after the first scan according to the clinical manifestation and rapid disease progression. This study was conducted in accordance with the amended Declaration of Helsinki. Local institutional review boards or independent ethics committees approved the protocol, and written informed consent was obtained from all patients.

Table 1
Radiographic characteristics of 195 patients diagnosed of COVID-19.

	Number (%)
Age	46 (33–59)
Sex	
Male	94 (48.2%)
Female	101 (51.8%))
Numbers of affected lobes	
Non	25 (12.8%)
Unilateral	26 (13.3%)
Bilateral	144 (73.8%)
1	22 (11.3%)
2	31 (15.9%)
3	26 (13.3%)
4	24 (12.3%)
5	67 (34.4%)
Location of the lesion	
Peripheral	162 (83.1%)
Central	8(4.1%)
GGO	80 (41.0%)
Solitary GGN/GGO	20 (10.3%)
Patchy ground-glass opacities	100 (51.3%)
Consolidation	89 (45.6%)
Increased vascular margins	123 (63.1%)
Long Axis Parallelism	109 (55.9%)
Nodule with halo sign	87 (44.6%)
Parenchymal band	84 (43.1%)
Reversed halo sign	62 (31.8%)
Air bronchogram	58 (29.7%)
Crazy paving	11 (5.6%)
Pleural effusion	6 (3.1%)
Mediastinal lymphadenopathy	2 (1.0%)

GGO, ground-glass opacification; GGN, ground-glass nodule.

2.3. Image interpretation analysis

All the images of 195 patients were anonymously reviewed by two radiologists separately and features were evaluated as follows: 1. Laterality and location of radiographic abnormalities. 2. Numbers of the lobes affected. 3. Ground-glass opacification (GGO): defined as an area of increased attenuation in the lung with preserved bronchial and vascular markings [16]. 4. solitary ground-glass nodule (GGN) or GGO. 5. Patchy ground-glass opacities. 6. Presence of consolidation. 7. Increased vascular margins on the central side of the lesion. 8. Long Axis Parallelism: defined as parallelism between the pleura and the long axis of the lesion. 9. Presence of nodule with halo sign. 10. Presence of parenchymal bands. 11. Presence of reversed halo sign. 12. Presence of air bronchogram. 13. Presence of crazy paving pattern: defined as the appearance of ground-glass opacity with superimposed interlobular septal thickening and intralobular septal thickening [17]. 14. Presence of mediastinal lymphadenopathy. 15. Presence of pleural effusion. 16. Progression assessment of the lesion based on CT scan which refers to: Stable, no change; Improving, decreased area and/or density of the lesion; Worsening, increased area and/or density of the lesion. We also collected laboratory test results including body temperature, complete blood cell (CBC) count, C-reactive protein (CRP), erythrocyte sedimentation rate (ESR), albumin and lactate dehydrogenase (LDH) level and analyzed comparison based on CT scan findings of total 187 patients.

Statistical analysis was performed with SPSS software. Quantitative data such as age was demonstrated as mean with 95% confidence interval, other counting data were present as the percentage of the total and analyzed with Person X^2 test. Significance was defined as a P value < 0.05.

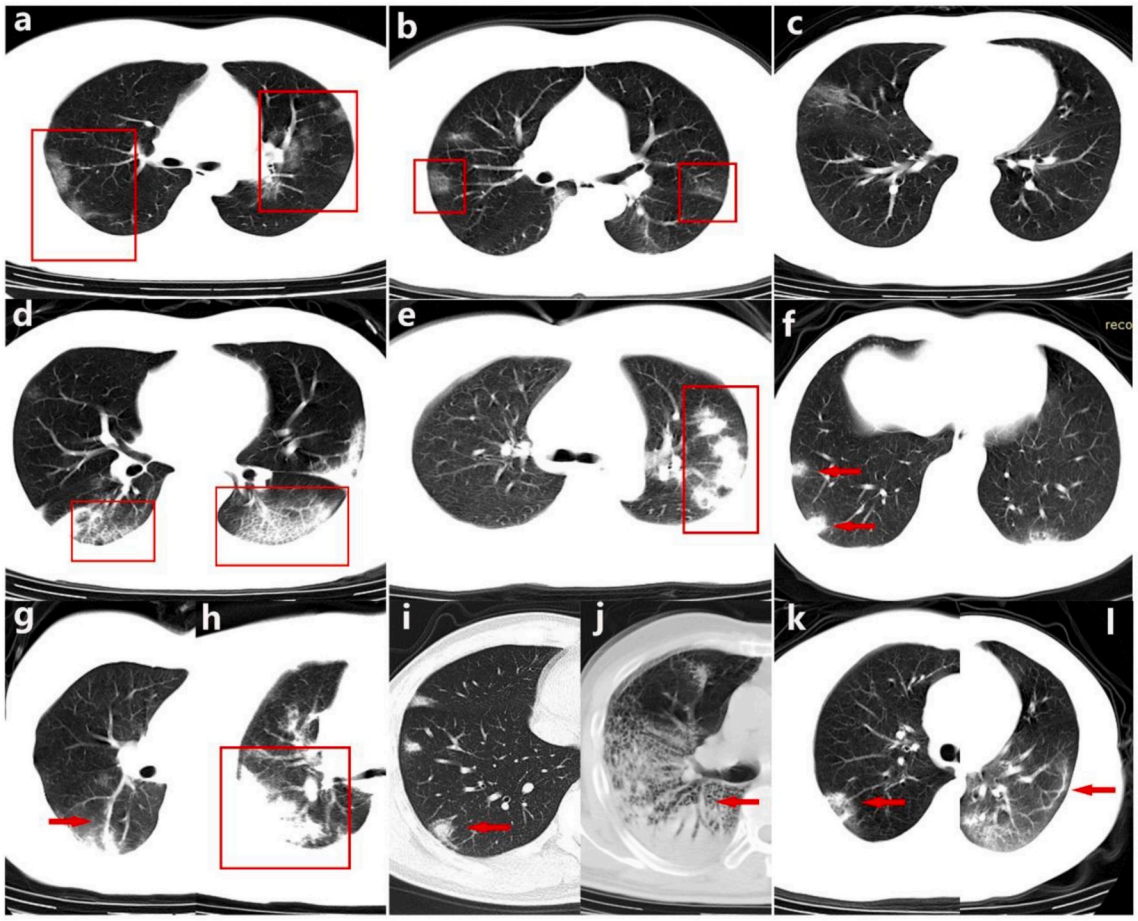

Fig. 1. Chest CT scan features of COVID-19. a-b. GGO. c. GGN. d. Crazy Paving Pattern. e. Long Axis Parallelism. f. Patchy Ground-glass Opacities. g. Increased Vascular Margins. h. Consolidation. i. Nodule with Halo Sign. j. Air Bronchogram. k. Reversed Halo Sign. l. Parenchymal Bands.

3. Results

3.1. General information

As shown in Table 1, the mean age of our study group is 46 years old (33–59) with no difference between male and female gender. The average duration from the initial symptom onset to the first CT scan was 10.9 days (2–39 days), and there were 95 patients had repeated CT scan after average 3.4 days (3–6 days).

3.2. Image characteristics on chest CT

There were 25(12.8%) confirmed cases reported no visible abnormalities at the first CT scan. 26(13.3%) cases present as unilateral lesion whereas 144(73.8%) present bilaterally. In terms of the number of affected lobes, 75.9% of the patients showed multiple lobes (≥2) involvements: 31(15.9%) cases of 2 lobes, 26(13.3%) of 3 lobes, 24 (12.8%) of 4 lobes and 67(34.2%) of 5 lobes. There were 22 (11.3%) cases showing lesion limited within one lobe. 83.1% (162 cases) of the total had peripheral distribution other than a central way (8 cases, 4.1%).

GGO was found in 80 (41.0%) patients and 20 cases (10.3%) present solitary GGN/GGO. Increased vascular margins on the central side of the lesion were noticed in 123 (63.1%) of the total cases. We also found 55.9% (109 cases) present parallelism between the pleura and the long axis of the lesion(Long Axis Parallelism), 51.3% (100 cases) showed patchy ground-glass opacities beneath the pleura, 45.6% (89 cases) with consolidations, 44.6% (87 cases) present nodules with surrounding halo sign and 43.1% (84 cases) with parenchymal bands (see Fig. 1).

In contrast, there were 31.8% (62 cases) present reversed halo sign, 29.7% (58 cases) with air bronchogram, 5.6% (11 cases) with crazy paving pattern, only 3.1% (6 cases) present with pleural effusion and 1% (2 cases) with mediastinal lymphadenopathy (LAD).

3.3. Time course

As shown in Table 2, we analyzed the evolution of different radiographic patterns according to the different duration from symptoms onset to the first CT scan, which defined as: super-early (1–3 days), early (4–7 days), intermediate (8–14 days) and late (over 15 days) stages.

Lesions trended to spread more bilaterally (41.7%–75.5%) and peripherally (50%–87.8%) from super-early to late stage. Furthermore, the number of the affected lobes also trended up along with the time course, 33.3% patients showed one lobe involvement at the super-early stage and 39.5% and 38.8% patients had total 5 lobes involvement at intermediate and late stage (Table 2).

Features such as increased vascular margins (50%, 66%, 63% and 63.3%) and nodules with halo signs (41.7%, 41.5%, 54.3% and 32.7%) appeared in the majority of the patients and there was no significant difference with the disease progression. In the intermediate stage, there was a decreased appearance of GGO followed by a rebounding rate at the late stage (41.7%, 45.3%, 27.2% and 59.2%). With which compared, the percentage of consolidation increased in the intermediate stage and subsided later on (33.3%, 45.3%, 58.0% and 28.6%). Along with consolidation, trending up followed by trending down was also noticed in features including air bronchogram (16.7%, 32.1%, 33.3% and

Table 2
Radiographic evolution of COVID-19 along with time course.

	No. (%)				P value
Duration	Super Early 1-3d (n = 12)	Early 4-7d(n = 53)	Intermediate 8-14d(n = 81)	Late ˃15d(n = 49)	
Age	50.6 ± 25.5	47.9 ± 18.3	43.5 ± 15.2	45.3 ± 14.2	0.345
Sex					
Male	7 (58.3%)	24 (45.3%)	36 (44.4%)	27 (55.1%)	0.577
Female	5 (41.7%)	29 (54.7%)	45 (55.6%)	22 (44.9%)	
Numbers of Affected Lobes					
Non	3 (25.0%)	6 (11.3%)	11 (13.6%)	5 (10.2%)	0.596
Unilateral	4 (33.3%)	11 (20.8%)	4 (4.9%)	7 (14.3%)	0.009
Bilateral	5 (41.7%)	36 (67.9%)	66 (81.5%)	37 (75.5%)	0.018
1	4 (33.3%)	9 (17.0%)	3 (3.7%)	6 (12.2%)	0.007
2	1 (8.3%)	9 (17.0%)	13 (16.0%)	8 (16.3%)	0.904
3	3 (25.0%)	6 (11.3%)	12 (14.8%)	5 (10.2%)	0.538
4	0 (0.0%)	8 (15.1%)	10 (12.3%)	6 (12.2%)	0.559
5	1 (8.3%)	15 (28.3%)	32 (39.5%)	19 (38.8%)	0.120
Location of the Lesion					
Peripheral	6 (50.0%)	44 (83.0%)	69 (85.2%)	43 (87.8%)	0.016
Central	3 (25.0%)	3 (5.7%)	1 (1.2%)	1 (2.0%)	0.007
GGO	5 (41.7%)	24 (45.3%)	22 (27.2%)	29 (59.2%)	0.004
Solitary GGN/GGO	4 (33.3%)	7 (13.2%)	5 (6.2%)	4 (8.2%)	0.027
Increased Vascular Margins	6 (50.0%)	35 (66.0%)	51 (63.0%)	31 (63.3%)	0.781
Nodule with Halo Sign	5 (41.7%)	22 (41.5%)	44 (54.3%)	16 (32.7%)	0.103
Consolidation	4 (33.3%)	24 (45.3%)	47 (58.0%)	14 (28.6%)	0.009
Air Bronchogram	2 (16.7%)	17 (32.1%)	27 (33.3%)	12 (24.5%)	0.519
Reversed Halo Sign	1 (8.3%)	14 (26.4%)	34 (42.0%)	13 (26.5%)	0.041
Patchy Ground-glass Opacities	2 (16.7%)	29 (54.7%)	45 (55.6%)	24 (49.0%)	0.082
Parenchymal Band	2 (16.7%)	18 (34.0%)	38 (46.9%)	26 (53.1%)	0.053
Long Axis Parallelism	4 (33.3%)	20 (37.7%)	52 (64.2%)	33 (67.3%)	0.002
Crazy Paving	1 (8.3%)	3 (5.7%)	4 (4.9%)	3 (6.1%)	0.870
Mediastinal LAD	0 (0.0%)	2 (3.8%)	0 (0.0%)	0 (0.0%)	0.255
Pleural Effusion	0 (0.0%)	1 (1.9%)	4 (4.9%)	1 (2.0%)	0.769

GGO, ground-glass opacification; GGN, ground-glass nodule; LAD, lymphadenopathy.

24.5%), patchy ground-glass opacities (16.7%, 54.7%, 55.6% and 49%), and reversed halo sign (8.3%, 26.4%, 42.0% and 26.5%).

We also found an increasing number of patients manifested as long axis parallelism (33.3%, 37.7%, 64.2% and 67.3%) and parenchymal bands (16.7%, 34.0%, 46.9% and 53.1%) during the evolution.

Low percentage of presence of crazy paving (8.3%, 5.7%, 4.9% and 6.1%), pleural effusion (0%, 1.9%, 4.9% and 2.0%) and mediastinal lymphadenopathy (0%, 3.8%, 0% and 0%) were noticed during the entire disease progression.

Table 3
COVID-19 progression assessments and correlation with radiographic features.

	Number		P value
Outcome	Improving or Stable	Worsening	
Number	80	15	
Age	45.3 ± 15.0	59.3 ± 13.5	**0.001**
Sex			
Male	37 (46.3%)	6 (40.0%)	0.655
Female	43 (53.8%)	9 (60.0%)	
Numbers of Affected Lobes			
Non	7 (8.8%)	0 (0.0%)	0.514
Unilateral	9 (11.3%)	0 (0.0%)	0.376
Bilateral	64 (80.0%)	15 (100%)	0.128
1	7 (8.8%)	0 (0.0%)	0.514
2	11 (13.8%)	2 (13.3%)	1.000
3	14 (17.5%)	2 (13.3%)	0.984
4	11 (13.8%)	4 (26.7%)	0.247
5	30 (37.5%)	7 (46.7%)	0.504
Location of the Lesion			
Peripheral	70 (87.5%)	14 (93.3%)	0.835
Central	3 (3.8%)	1 (6.7%)	0.503
GGO	34 (42.5%)	7 (46.7%)	0.765
Solitary GGN/GGO	8 (10.0%)	0 (0.0%)	0.439
Patchy Ground-glass Opacities	42 (52.5%)	9 (60.0%)	0.593
Consolidation	39 (48.8%)	8 (53.3%)	0.745
Increased Vascular Margins	45 (56.3%)	9 (60.0%)	0.788
Long Axis Parallelism	50 (62.5%)	8 (53.3%)	0.504
Nodule with Halo Sign	38 (47.5%)	5 (33.3%)	0.312
Parenchymal Band	39 (48.8%)	7 (46.7%)	0.882
Reversed Halo Sign	28 (35.0%)	5 (33.3%)	0.901
Air Bronchogram	23 (28.7%)	7 (46.7%)	0.286
Crazy Paving	5 (6.3%)	3 (20.0%)	0.210
Pleural Effusion	2 (2.5%)	0 (0.0%)	1.000
Mediastinal LAD	1 (1.3%)	0 (0.0%)	1.000

GGO, ground-glass opacification; GGN, ground-glass nodule; LAD, lymphadenopathy.

3.4. Progression assessment

As shown in Table 3, the progression assessments along with time course were analyzed, 64 (67.4%) patients showed improvements on CT scan (Fig. 2a and b), 15 (15.8%) showed worsening manifestation (Fig. 2c and d) and 16 (16.8%) present as stable. Compared with worsening group, we found that patients tended to have younger age in improving/stable group (45.3 ± 15.0 VS. 59.3 ± 13.5, P = 0.001). There was no significant difference between worsening group and improving/stable group regarding all the characteristics shown on the first CT scan (Table 3).

3.5. Correlation between laboratory test abnormalities and CT scan findings

Table 4 has showed the laboratory test results among 187 patients of the total and the correlation with CT scan. Mean age was 43(32.0–58.0) years old and mean WBC count was 4.69×10^9/L (95% CI $3.62–5.78\times10^9$/L), in which the percentage of neutrophil, lymphocyte and monocytes were 63.2% (55.3–71.9%), 27.3% (19.9–35.2%), and 7.5% (6.0–9.1%) respectively. Levels of LDH (U/L), albumin (g/L), CRP (mg/L) and ESR (mm/h) were 168.4 (141.1–215.5), 37.66 (35.19–40.38), 15.69 (4.93–29.85) and 40.0 (22.0–67.3) respectively. We have found a significant difference between the positive and negative CT finding groups. As shown in Table 4, patients with positive CT findings shared elder age, 46.0 (35.0–60.0)VS.31.0 (12.0–37.0) $P < 0.001$, and higher chance developing fever($P < 0.05$); higher level of lymphocytes, CRP, ESR and LDH; lower level of WBC, neutrophil and albumin($P < 0.001$).

4. Discussion

In our study, we have collected both clinical and image data of nearly

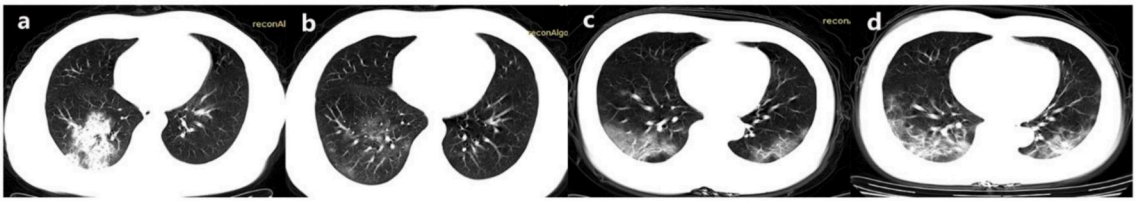

Fig. 2. Radiographic comparison between the first and second CT scan 3 days later. 2a-b. Decreased area and density of GGO. 2c-d. Increased area and density of GGO.

Table 4
Correlation between laboratory test results and CT scan findings.

Characteristic	All Patients	Positive CT	Negative CT	P value
Number	187	164	23	
Age	43.0 (32.0–58.0)	46.0 (35.0–60.0)	31.0 (12.0–37.0)	**<0.001**
Fever (°C)				
˃39.0	13 (7.0%)	12 (7.3%)	1 (4.3%)	**0.033**
38.1 to 39.0	62 (33.2%)	60 (36.6%)	2 (8.7%)	
37.3 to 38.0	63 (33.7%)	53 (32.3%)	10 (43.5%)	
<37.3	49 (26.2%)	39 (23.8%)	10 (43.5%)	
Laboratory Findings		+	−	
WBC (*10^9/L)	4.69 (3.62–5.78)	4.62 (3.59–5.66)	6.06 (4.15–7.73)	**0.009**
Neutrophil %	63.2 (55.3–71.9)	64.8 (56.7–73.0)	53.3 (46.1–60.7)	**<0.001**
Lymphocyte %	27.3 (19.9–35.2)	25.9 (18.5–32.7)	38.6 (29.2–43.7)	**<0.001**
Albumin (g/L)	37.66 (35.19–40.38)	36.91 (34.38–39.84)	42.01 (39.17–43.35)	**<0.001**
LDH (U/L)	168.4 (141.1–215.5)	174.0 (142.8–224.4)	145.4 (110.2–164.4)	**<0.001**
CRP (mg/L)	15.69 (4.93–29.85)	18.60 (8.30–31.61)	2.88 (2.36–5.30)	**<0.001**
ESR (mm/h)	40.0 (22.0–67.3)	50.0 (25.5–72.5)	22.0 (10.5–27.5)	**<0.001**

WBC, white blood cell; LDH, lactate dehydrogenase; CRP, C-reactive protein; ESR, erythrocyte sedimentation rate.

200 cases from December 31, 2019 to February 20, 2020 in First Hospital of Changsha, the only designated hospital for admission and management of COVID-19 patients from Changsha and surrounding area. According to the official announcement of National Health Commission of China, there were totally 242 cases confirmed with COVID-19 by March 9, 2020 (http://www.nhc.gov.cn/xcs/yqfkdt/202003/948a03ad76f54d3583a018785efd7be9.shtml). The integrity and representativeness of our study illustrated a comprehensive knowledge of COVID-19 based on the radiographic feature and clinical manifestation.

Zhe Xu's team [18] has reported the pathological findings of COVID-19 patients including bilateral diffuse alveolar damage with cellular fibromyxoid exudates, desquamation of pneumocytes, edema and hyaline membrane formation, indicating the presence of acute respiratory distress syndrome (ARDS). The interstitial mononuclear inflammatory infiltration, multinucleated syncytial cells with atypical enlarged pneumocytes characterized by large nuclei, amphophilic granular cytoplasm, and prominent nucleoli were also identified in the intra-alveolar spaces, indicating viral cytopathic-like changes.

GGO is commonly seen in many inflammatory diseases such as atypical pneumonia (viral/mycoplasmal/pneumocystis pneumonia), ARDS, pulmonary edema or pulmonary hemorrhage [19]. The pathophysiological mechanism is due to interstitial or alveolar wall thickening secondary to inflammatory reaction, partial filling of air space, or increased capillary blood flow [20,21]. The halo sing around nodules and increased vascular margins on the central side of the lesion shared the same underlying pathophysiology. The latter characteristic, additionally, also indicated vascular involvements due to the expression of angiotensin-converting enzyme 2 (ACE2) on the cell surface membrane of vascular endothelial cells. Our study revealed high percentage of these features from the super-early to late stage, suggesting the inflammatory cells infiltration, interstitial damage and exudation prolonged during the disease evolution.

Consolidation occurrence peaked in the intermediate stage and declined subsequently, which correlated with inflammatory infiltration and exudative accumulation. On the contrary, GGO occurrence was found a drop in intermediate stage and rebounded in late stage because of the absorption of consolidation, indicating underlying recovery. The same trend could also be noticed in reversed halo sign and air bronchogram, corresponding to alveolar septal inflammation and cellular debris in alveolar spaces surrounded by ring-shaped or crescent consolidation. As the disease progresses, the affected area spread more peripherally, forming a parallelism between the pleura and the long axis of the lesion, and more parenchymal bands were noticed, indicating that early inflammation was gradually absorbed and replaced by fibroid recovery along with the disease evolution. Additionally, long axis parallelism may correlate with the virus spreading within alveolar epithelial cells, which diffusely located in the peripheral area and facilitated SARS-CoV2 infusion due to large amount of ACE2 expression on the cellular surface membrane.

We have assessed the radiographic progression based on the features of first CT scan and found that younger aged patients tended to have higher rate of improvement or stabilization. On the other hand, no relationship was found between radiographic characteristics and outcomes, indicating that none of the CT scan features had predictive value statistically. However, relatively higher percentage of bilateral and multiple lobes (≥3) involvements were noticed in the worsening group accordingly. As a result, decision should be made comprehensively based on image tests, laboratory results and clinical symptoms when making further management strategy.

In 187 cases, we have found that patients with positive findings of COVID-19 shared elder age, higher rate of fever, higher level of neutrophils, CRP, ESR and LDH; lower level of WBC, lymphocytes and albumin($P < 0.001$). Suggesting a positive correlation between the systemic inflammation level and radiographic characteristics, consisting with clinical evolution of COVID-19.

There were several limitations of our study. First, because of the short time for data collection, there were only 95 of 195 patients had repeated CT scan and a lack of subsequent image follow-up. Second, the slice thickness of our CT scan was 5 mm which might have relatively low sensitivity for certain radiological features such as crazy paving, interlobular septal thickening and air bronchogram. At last, there was a lack of severity analysis of our cases. Our study had shown that radiographic worsening tended to happen among elderly group but could not be able to show a correlation between the critical ill patients and radiographic evolution.

In conclusion, our study had manifested several certain radiographic characteristics of COVID-19 which may be helpful for the early recognition and differential diagnosis. We also showed a correlation between radiographic feature and laboratory test results and revealed an intact picture of COVID-19.

Funding

This work was supported by the "Gaoyuan" project of Pudong Health and Family Planning Commission [PWYgy2018-6] of Shanghai and National Key Research and Development Program of China [2018YFC1313700] for the acquisition, analysis and interpretation of data.

Declaration of competing interest

None.

CRediT authorship contribution statement

Zhibing Luo: Writing - original draft, Writing - review & editing. **Na Wang:** Writing - original draft, Writing - review & editing. **Ping Liu:** Data curation. **Qian Guo:** Writing - original draft, Writing - review & editing. **Linyu Ran:** Data curation. **Feilong Wang:** Writing - review & editing, Formal analysis. **Yuling Tang:** Conceptualization. **Qiang Li:** Conceptualization.

Acknowledgements

We would like to thank all the patients and health care workers devoted themselves into this COVID-19 outbreak.

Appendix A. Supplementary data

Supplementary data to this article can be found online at https://doi.org/10.1016/j.rmed.2020.105989.

References

[1] N. Zhu, et al., A novel coronavirus from patients with pneumonia in China, N. Engl. J. Med. (2019), https://doi.org/10.1056/NEJMoa2001017, 2020.
[2] Organization, W.H, Novel Coronavirus (2019-nCoV): Situation Report-22, 2020. Feb.11.
[3] Organization, W.H, Coronavirus Disease 2019 (COVID-19) Situation Report – 87, 2020. Apr.16.
[4] Organization, W.H, Coronavirus Disease 2019 (COVID-19) Situation Report – 39, 2020. Feb.28.
[5] Q. Li, et al., Early transmission dynamics in Wuhan, China, of novel coronavirus-infected pneumonia, N. Engl. J. Med. (2020), https://doi.org/10.1056/NEJMoa2001316.
[6] W.J. Guan, et al., Clinical characteristics of coronavirus disease 2019 in China, N. Engl. J. Med. (2020), https://doi.org/10.1056/NEJMoa2002032.
[7] Chen, N., et al, Epidemiological and clinical characteristics of 99 cases of 2019 novel coronavirus pneumonia in Wuhan, China: a descriptive study. Lancet.doi: 10.1016/S0140-6736(20)30211-7.
[8] Z. Wu, J.M. McGoogan, Characteristics of and important lessons from the coronavirus disease 2019 (COVID-19) outbreak in China: summary of a report of 72314 cases from the Chinese center for disease control and prevention, Jama (2020), https://doi.org/10.1001/jama.2020.2648.
[9] Lancet, Clinical features of patients infected with 2019 novel coronavirus in Wuhan, China. Lancet 2020; published online Jan 24. - Correction, Lancet 395 (10223) (2020) 496, https://doi.org/10.1016/S0140-6736(20)30252-X.
[10] D. Wang, et al., Clinical characteristics of 138 hospitalized patients with 2019 novel coronavirus-infected pneumonia in Wuhan, China, J. Am. Med. Assoc. (2020), 10.1001/jama.2020.1585.doi:10.1001/jama.2020.1585.
[11] A. Bernheim, et al., Chest CT findings in coronavirus disease-19 (COVID-19): relationship to duration of infection, Radiology (2020) 200463, https://doi.org/10.1148/radiol.2020200463.
[12] Y. Chen, Q. Liu, D. Guo, Emerging coronaviruses: genome structure, replication, and pathogenesis, J. Med. Virol. (2020), https://doi.org/10.1002/jmv.25681.
[13] R. McBride, M. van Zyl, B.C. Fielding, The coronavirus nucleocapsid is a multifunctional protein, Viruses 6 (8) (2014) 2991–3018, https://doi.org/10.3390/v6082991.
[14] J.F. Chan, et al., A familial cluster of pneumonia associated with the 2019 novel coronavirus indicating person-to-person transmission: a study of a family cluster, Lancet 395 (10223) (2020) 514–523, https://doi.org/10.1016/s0140-6736(20)30154-9.
[15] Organization, W.H, Laboratory Testing for 2019 Novel Coronavirus (2019-nCoV) in Suspected Human Cases, W.H. Organization, 2020. Feb.17.
[16] J.H. Austin, et al., Glossary of terms for CT of the lungs: recommendations of the nomenclature committee of the Fleischner society, Radiology 200 (2) (1996) 327–331, https://doi.org/10.1148/radiology.200.2.8685321.
[17] W. De Wever, et al., The crazy-paving pattern: a radiological-pathological correlation, Insights Imaging 2 (2) (2011) 117–132, https://doi.org/10.1007/s13244-010-0060-5.
[18] Z. Xu, et al., Pathological findings of COVID-19 associated with acute respiratory distress syndrome, Lancet Respir Med (2020), https://doi.org/10.1016/s2213-2600(20)30076-x.
[19] L. Bessis, et al., High-resolution CT of parenchymal lung disease: precise correlation with histologic findings, Radiographics 12 (1) (1992) 45–58, https://doi.org/10.1148/radiographics.12.1.1734481.
[20] A.N. Leung, R.R. Miller, N.L. Muller, Parenchymal opacification in chronic infiltrative lung diseases: CT-pathologic correlation, Radiology 188 (1) (1993) 209–214, https://doi.org/10.1148/radiology.188.1.8511299.
[21] M. Remy-Jardin, et al., Computed tomography assessment of ground-glass opacity: semiology and significance, J. Thorac. Imag. 8 (4) (1993) 249–264, https://doi.org/10.1097/00005382-199323000-00001.